A heterocyclic compound 5-acetyl-2,4-dimethylthiazole, spectroscopic, natural bond orbital, nonlinear optical and molecular docking studies

D. Avcı[a], B. Dede[b,*], S. Bahçeli[c], and D. Varkal[c]

[a]*Department of Physics, Faculty of Arts and Science, Sakarya University, Sakarya, Turkey.*
[b]*Department of Chemistry, Faculty of Arts and Science,*
Süleyman Demirel University, East Campus, 32260, Isparta, Turkey.
e-mail: bulentdede@sdu.edu.tr
[c]*Department of Physics, Faculty of Arts and Science,*
Süleyman Demirel University, East Campus, 32260, Isparta, Turkey.

In this work, the 5-acetyl-2,4-dimethylthiazole (C_7H_9NSO) molecule was studied by using the experimental UV-vis (in three different solvents) and FT-IR spectral results, and theoretically using DFT calculation method. The calculated molecular geometric parameters, vibrational wavenumbers, HOMO-LUMO energies, ^1H and ^{13}C NMR chemical shift values, natural bond orbitals, and nonlinear optical properties of the 5-acetyl-2,4-dimethylthiazole (C_7H_9NSO) molecule at the B3LYP/ and HSEH1PBE/6-LanL2DZ levels of the theory. The spectral results obtained from the quantum chemical calculations of the title compound are in a good agreement with the experimental results. Additionally, molecular docking studies were carried out to show vascular endothelial growth factor and β-ketoacyl-acyl carrier protein synthase III inhibitory effect of 5-acetyl-2,4-dimethylthiazole. Molecular docking studies indicated that 5-acetyl-2,4-dimethylthiazole has potency to be used as an antiproliferative and antibacterial agent.

Keywords: 5-Acetyl-2,4-dimethylthiazole; FT-IR and UV-vis spectroscopies; ^1H and ^{13}C NMR chemical shifts; DFT method; molecular docking.

PACS: 07.60.Rd; 33.20.Tp; 31.15.E-; 42.65.-k

1. Introduction

Cancer is a group of more than 100 diseases that are formed by the uncontrolled proliferation of cells in various parts of our body. Untreated cases may result in serious discomfort or even death. The uncontrolled and rapid proliferation of cancer cells is due to the fact that the activity or number of growth factor receptors is excessively high. Among these factors, vascular endothelial growth factor (VEGFR-2) is a transmembrane receptor that plays an important role in endothelial cell development [1,2] and is thought to mediate the key effects of the endothelial-specific mitogen VEGF on cell proliferation and permeability. Therefore, the majority of VEGFR-2 actions are related to angiogenesis, which is one of the critical processes that affect growth and development of cancerous cells [3,4]. Blocking VEGFR-2 signalling pathway has become an attractive approach for the treatment of cancer [5,6]. Vatalanib (PTK787/ZK-222584), Semaxanib (SU5416), Sorafenib (BAY 43-9006), Vandetanib (ZD6474), Sunitinib (SU11248) are some of the antiangiogenic molecules that inhibit all vascular endothelial growth factor receptors. As the pharmaceutical field continues to evolve, efforts are underway to find new and effective VEGFR-2 inhibitors and development of different, and more effective anti-cancer agents than the known drugs is very important. The thiazoles in this area are a little more foreground and in the field of medicinal chemistry, thiazoles are of great interest since they are highly biologically active compounds, including numerous natural products and pharmaceutical agents [7,8].

Antibiotics are drugs used in the treatment of bacterial infection diseases, and are very important in terms of human health. the discovery of antibiotics in the last century decreased the infectious disease dependent deaths in a great extent. However, the increase in antibacterial resistance among bacterial pathogens is a worldwide thread constraining the different potential antibacterials. In the majority of existing pathogenic bacteria, this resistance to drugs is constantly emerging. Therefore, it is very important to have alternative agents that can be used as new antibacterial agents to prevent this serious problem. β-Ketoacyl-acyl carrier protein (ACP) synthase III (KAS III, also called acetoacetyl-ACP synthase) encoded by the FabH gene is thought to catalyze the first elongation reaction (Claisen condensation) of type II fatty acid synthesis in bacteria and plant plastids [9]. Biological activity of 5-acetyl-2,4-dimethylthiazole was also evaluated as potential inhibitors of *Escherichia coli (E. coli)* FabH with antibacterial activity.

Molecular structure states almost everything about the molecular function, if desired in detail. For a candidate anticancer and antibacterial agent, stability, softness and hardness, electronic behaviour and bonding capacity have to be well known. DFT study B3LYP exchange correlation functional gives structural and spectroscopic informations about the molecule which can be bridged to the function. In this framework, the B3LYP (Becke's three-parameter exact exchange functional (B3) combined with the gradient-corrected correlational functional of Lee, Yang, and Parr (LYP)) hybrid method and the HSEH1PBE (it is deciphered as the Heyd-

Scuseria-Ernzerhof hybrid combined with Perdew, Burke, and Ernzerhof's exchange and correlation functions), called the HSE06 approach basis sets, are often used as adequate basis sets in the density functional theory (DFT) as a quantum chemical calculation method [10-18].

Very recently, in our previous work, 2-ethoxythiazole (C_5H_7NSO) compound as the member of five-membered ring with one nitrogen atom group was investigated by using the spectroscopic and DFT methods for the first time [19]. 5-Acetyl-2,4-dimethylthiazole molecule (C_7H_9NSO) is now studied with the same framework, that is, in terms of spectroscopic, DFT quantum chemical calculations and molecular docking studies, since it can also be found worth of investigation by considering its biological properties, and the lack of its spectroscopic and quantum chemical studies in the literature according to our best knowledge.

At the present work, the experimental FT-IR and UV-vis (in chloroform, ethanol and N,N-dimethylformamide solvents) spectral results, the molecular geometry, the simulated vibrational and UV-vis (in gase phase and chloroform solvent) spectra, the proton and carbon-13 NMR chemical shift values, HOMO-LUMO, NBO analyses and NLO properties were calculated using DFT/B3LYP and HSEH1PBE with LanL2DZ which stands for "Los Alamos National Laboratory 2-Double-Z" basis set. Furthermore based on the above consideration, we performed molecular docking studies into the active sites of VEGFR-2 kinase and KAS III.

2. Experimental

5-Acetyl-2,4-dimethylthiazole (99%, Alfa Aesar), chloroform (99%, Merck), ethanol (99.9%, Merck) and N,N-dimethylformamide (99.8%, Merck) used in this work were obtained from commercial sources, and were used without any purification. IR spectrum of the 5-acetyl-2,4-dimethylthiazole was recorded at room temperature on a Schimadzu IR Prestige-21 FT-IR (Fourier Transform Infrared) Spectrometer with a resolution of 4 cm^{-1} in the transmission mode. The prepared samples were compressed into self-supporting pellet and introduced into an IR cell equipped with KBr window. PG Instrument T80+ ultraviolet spectrophotometer was used to record the ultraviolet visible spectrum of the title compound at room temperature. The ultraviolet visible spectra of the mentioned compound solved in chloroform, ethanol and N,N-dimethylformamide solvents were verified with spectral bandwidth 2 nm and quartz cell 1 cm.

2.1. Computational details

All calculations were carried out using Gaussian 09 program package with the GaussView 05 molecular visualization program on personal computer [20,21]. The molecular structure and vibrational computations of 5-acetyl-2,4-dimethylthiazole molecule were calculated by using Becke-3-Lee Yang Parr (B3LYP) and HSEH1PBE density functional theory methods with LanL2DZ basis set in ground state, respectively. Since the other well-known basis set lead us to imaginary vibrational frequency values, the mentioned basis set was used, and so the optimized molecular structure of title molecule in the ground state was obtained at the B3LYP/ and HSEH1PBE/ LanL2DZ levels. By considering the well-known systematic errors which come from the negligence of anharmonicity, electron correlation and basis set deficiencies, and furthermore, the computation in DFT method was performed in gas phase of isolated molecule while the experimental measurements were taken in solid phase for the title molecule [22,23], the calculated vibrational wavenumbers were scaled as 0.961 for frequencies higher than 800 cm^{-1} and 1.001 for frequencies less than 800 cm^{-1} at the B3LYP and HSEH1PBE/LanL2DZ levels [24]. The assignments of fundamental vibrational modes of the title molecules were performed on the basis of total energy distribution (TED) analysis by using VEDA 4 program [25]. In the NMR calculations, the optimized molecular geometry of title molecule was first obtained at the B3LYP and HSEH1BPE/LanL2DZ levels for 5-acetyl-2,4- dimethylthiazole, by using the conductor-like polarizable continuum method (CPCM). Afterwards, the ^{1}H and ^{13}C NMR chemical shifts were calculated using the gauge- including atomic orbital (GIAO) method based on optimized at the mentioned levels in gas phase and in CHCl$_3$ solvent [26,27]. The UV-vis spectra in gas phase and chloroform solvent were obtained using the time dependent DFT (TD-DFT) method. [28,29] Furthermore, the FMO analyses of the title compound were performed by using DFT/HSEH1PBE method with 6-311++G(d,p) basis set and their 3D plots were verified.

2.2. Molecular Docking

Molecular docking studies of 5-acetyl-2,4-dimethylthiazole was performed by on SwissDock web server using EADock DSS algorithm [30]. High resolution crystal structure of vascular endothelial growth factor (VEGFR-2) (PDB ID: 2XIR) and β-ketoacyl-acyl carrier protein (ACP) synthase III (KAS III) (PDB ID: 1HNJ) were downloaded from a protein data bank website (https://www.rcsb.org/pdb/home/home.do). 5-Acetyl-2,4-dimethylthiazole was prepared for docking by energy minimized using the molecular mechanics and the semi-empirical AM1 methods with Gaussian 09 program package [20]. All images in molecular docking studies were drawn with the UCSF Chimera package [31].

3. Results and Discussion

3.1. Molecular structure

The optimized molecular structures at the HSEH1PBE/Lan L2DZ levels basis set of the 5-acetyl-2, 4-dimethylthiazole

TABLE I. The calculated bond lengths (Å), bond angles and dihedral angles (°) for 5-acetyl-2,4-dimethylthiazole at the B3LYP and HSEH1PBE/LanL2DZ levels.

| Parameters	B3LYP	HSEH1PBE
Bond lengths		
C1-S4	1.8141	1.8001
C1-N5	1.3203	1.3171
C1-C11	1.4991	1.4906
C2-C3	1.3937	1.3893
C2-N5	1.4025	1.3952
C2-C6	1.5094	1.5005
C3-S4	1.8203	1.8060
C3-C10	1.4755	1.4685
C10-C15	1.5227	1.5126
C10-O19	1.2588	1.2539
Bond angles		
S4-C1-N5	114.2158	114.3176
S4-C1-C11	121.5027	121.4847
N5-C1-C11	124.2814	124.1977
C3-C2-N5	114.7115	114.614
C3-C2-C6	128.6948	128.6239
N5-C2-C6	116.5937	116.762
C2-C3-S4	110.2424	110.3151
C2-C3-C10	132.679	132.6023
S4-C3-C10	117.0786	117.0827
C1-S4-C3	87.3958	87.5172
C1-N5-C2	113.4344	113.2361
C3-C10-C15	119.8574	119.6661
C3-C10-O19	119.9356	119.9199
C15-C10-O19	120.207	120.414
Dihedral angles		
N5-C1-S4-C3	0.0013	0.0033
C11-C1-S4-C3	179.9998	180.0011
S4-C1-N5-C2	-0.0008	-0.0023
C11-C1-N5-C2	-179.9993	-180.0
N5-C2-C3-C10	180.0008	-179.9982
C6-C2-C3-S4	180.0004	-179.9988
C6-C2-C3-C10	0.0	0.0
C3-C2-N5-C1	-0.003	-0.0005
C6-C2-N5-C1	179.9989	-179.999
C2-C3-S4-C1	-0.0014	-0.0034
C10-C3-S4-C1	179.9983	179.9976
C2-C3-C10-C15	0.0017	-0.0009
C2-C3-C10-O19	179.9983	-179.9976
S4-C3-C10-C15	180.0012	179.9978
S4-C3-C10-O19	-0.0021	0.0012
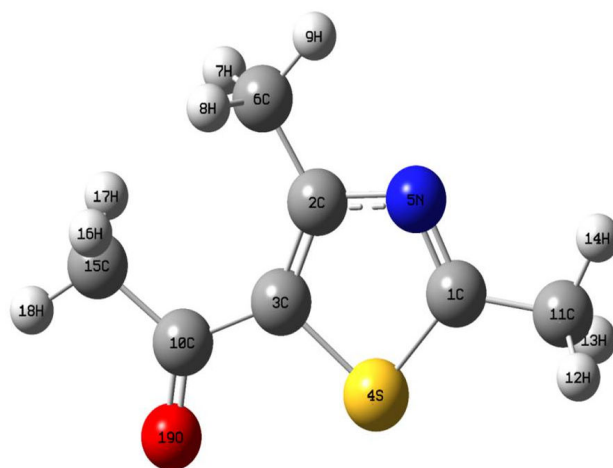
FIGURE 1. The optimized molecular geometry of 5-acetyl-2,4-dimethylthiazole at the B3LYP/LanL2DZ level.

compound are in Fig. 1. In Table I we only present some selected bond lengths, bond angles and dihedral angles which were calculated at the B3LYP and HSEH1BPE /LanL2DZ levels for the title molecule.

By considering the Table I and Fig. 1, in thiazole ring the double bond C1=N5 and the single bond C2-5N were calculated as 1.3203/1.3171 and 1.4025/1.3952 Å at the B3LYP and HSEH1BPE /LanL2DZ levels, respectively. Likewise, the bond lengths C1-S4 and C3-S4 were found as 1.8141/1.8001 and 1.8203/1.806 Å at the mentioned levels, respectively, which are the longest bond lengths of the title molecule. On the other hand, in CH$_3$CO- acetyl group of the 5-acetyl-2,4-dimethylthiazole compound, the double carbonyl C10=O19 bond length was calculated as 1.2588/1.2239 Å at the mentioned levels, respectively which are the shortest bond length of the title molecule. Furthermore, in the thiazole ring of the title compound the calculated S4-C1-N5, C1-S4-C3 and C1-N5-C2 bond angle values were found as 114.2158/114.3176, 87.3958/87.5172 and 113.4344/113.3176° while the C3-C10-O19 bond angle in the CH$_3$CO- acetyl group were calculated as 119.9356/119.9199° at the mentioned levels, respectively, as seen in Table I. Likewise, by considering some selected dihedral angles of the title compound exhibited in Table I, we should express that the compound under investigation is a non-planar molecule.

3.2. Vibrational analysis

The experimental and simulated IR spectra of the 5-acetyl-2,4-dimethylthiazole compound (C$_7$H$_9$NOS) are shown in Fig. 2. This molecule has 19 atoms, and its number of fundamental vibrational modes is 51. Furthermore, the observed and calculated at the B3LYP and HSEH1BPE/LanL2DZ levels vibrational frequencies and vibrational frequency assignments of the title compound are summarized in Table II. As seen in Table II, the assignments of vibrational frequencies were performed by using PED analysis.

TABLE II. Comparison of FT-IR and calculated vibration frequencies for the 5-acetyl-2,4-dimethylthiazole.

Mode	Assignments via PED% at HSEH1PBE level	FT-IR [cm^{-1}]	Scaled freq. [cm^{-1}]^a	
			B3LYP	HSEH1PBE
1	ν(CH) 97%		3058.49	3089.61
2	ν(CH) 78%		3052.72	3084.05
3	ν(CH) 98%		3049.44	3083.68
4	ν(CH) 100%		3017.11	3049.69
5	ν(CH) 100%	2999.31	3008.94	3042.80
6	ν(CH) 100%	2964.59	3004.72	3039.31
7	ν(CH) 79%	2961.56	2938.89	2961.81
8	ν(CH) 80%		2935.95	2960.55
9	ν(CH) 100%	2924.08	2932.77	2957.62
10	ν(OC) 80%	1670.31	1560.83	1595.54
11	ν(NC) 13%+ν(CC) 51%	1510.28	1498.29	1528.25
12	ν(NC) 45%+ν(CC) 26%		1475.42	1500.61
13	β(HCH) 60%+τ(HCCC) 14%		1467.75	1473.16
14	β(HCH) 61%		1454.79	1461.08
15	ν(NC) 35% +β(HCH) 19%	1446.61	1444.87	1448.45
16	β(HCH) 48%+τ(HCCC) 11%		1443.66	1447.39
17	ν(NC) 10% +β(HCH) 69%		1432.61	1441.51
18	β(HCH) 62%		1426.83	1427.95
19	β(HCH) 87%		1388.61	1392.94
20	β(HCH) 94%		1386.64	1390.82
21	β(HCH) 86%	1371.39	1366.00	1371.08
22	ν(CC) 42% +β(CCN) 24%	1317.38	1295.79	1326.23
23	ν(NC) 37%+ν(CC) 22%	1269.52	1223.73	1252.40
24	ν(CC) 27%+β(CNC) 12%+?(CCN) 12%+?(HCCS) 22%	1182.38	1149.78	1170.30
25	ν(CC) 12% +τ(HCCC) 20%	1056.99	1044.35	1057.36
26	τ(HCCC) 47%+γ(CCNC) 10%	1041.58	1041.12	1046.04
27	β(HCH) 20%+τ(HCCS) 58%		1030.12	1034.66
28	ν(NC) 12%+τ(HCCC) 20%		1021.25	1031.93
29	τ(HCCC) 45%+γ(OCCC) 20%	1016.49	1016.58	1021.55
30	ν(NC) 10%+ν(CC) 12%+τ(HCCC) 20%	958.62	976.74	991.25
31	ν(NC) 18%+ ν(CC) 11%	931.62	925.18	938.16
32	ν(CC) 41%+β(CCN) 12%+ β(CNC) 18%		860.45	885.11
33	τ(HCCC) 18%+τ(CCNC) 30%+γ(CCSC) 14%	686.66	691.43	698.30
34	ν(SC) 21% +ν(CC) 12%+ β(CCN) 15%+β(SCN) 21%	667.37	667.11	678.55
35	ν(SC) 39% + β(CCN) 11%+β(SCN) 12%		636.74	656.33
36	τ(HCCC) 20%+τ(SCNC) 15%+γ(OCCC) 31%		618.39	624.61
37	β(OCC) 36%+ β(CNC) 21%	598.29	579.54	588.89
38	ν(CC) 21%+ν(SC) 18% +β(OCC) 15%+β(CNC) 12%	567.07	558.12	570.49
39	τ(SCNC) 32%+γ(OCCC) 12%+ γ(CSNC) 19%	547.78	512.61	519.01
40	β(CCC) 17%+β(SCN) 43%	453.27	474.23	483.09
41	ν(CC) 12%+β(CCN) 47%		352.27	355.78
42	β(CCN) 17%+ β(OCC) 13%+ β(CCC) 40%		327.45	329.70
43	τ(SCNC) 11%+γ(CSNC) 22%+ γ(CCSC) 36%		296.21	299.09
44	β(CNC) 10%+ β(CCN) 74%		282.40	284.30
45	τ(HCCC) 25%+γ(CSNC) 13%		219.32	227.18
46	τ(CCNC) 27%+ γ(CCNC) 41%		195.99	199.98
47	β(CCS) 65%+ β(CCC) 15%		182.61	182.08
48	τ(CCNC) 16%+τ(SCNC) 24%+?(CSNC) 11%+ ?(CCSC) 31%		112.89	114.09
49	τ(HCCC) 15%+τ(CCCC) 55%		68.63	69.90
50	τ(HCCS) 84%+γ(CSNC) 12%		49.29	44.26
51	β(HCC) 26%+τ(HCCC) 22%+τ(CCCC) 28%		46.07	41.06

ν: Stretching; β: in plane bending; γ: out of plane bending; τ: twisting^a. The calculated vibrational frequencies of 5-acetyl-2,4-dimethylthiazole were scaled as 0.961 for frequencies higher than 800 cm^{-1} and as 1.001 for frequencies lower than 800 cm^{-1} at the B3LYP and HSEH1PBE/LanL2DZ levels.
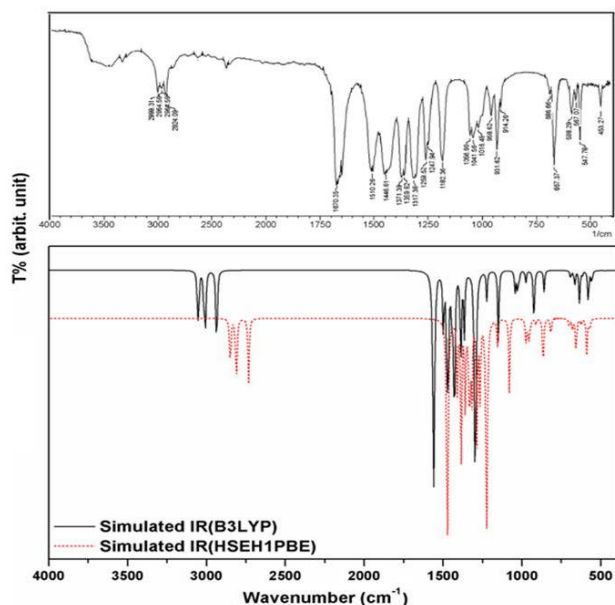
FIGURE 2. The experimental and simulated IR spectra of 5-acetyl-2,4-dimethylthiazole.

By considering Table II and Fig. 2, the $\nu(CH)$ symmetric stretching modes of the title molecule are observed at 2999.31, 2964.59, 2924.08 and 2961.56 cm^{-1} while their calculated wavenumber values at the B3LYP and HSEH1PBE/LanL2DZ level were found as 3008.94/3042.80, 3004.72/3039.31, 2932.77/2957.62 and 2938.89/2961.81 cm^{-1} which are the quite pure modes by the 100% and 79% PED contributions, respectively [32-36]. On the other hand, the position of C=O stretching band at the interval 1870-1540 cm^{-1} depends on properties such as the physical state, electronic and mass effects of neighboring substituents, intramolecular and intermolecular hydrogen bonding and conjugations [33,34]. In this context, the C=O stretching band of the title molecule is observed at 1670.35 cm^{-1} as a very strong band as seen in Fig. 2, and its calculated value at the mentioned levels were found as 1560.83/1595.54 cm^{-1} which shows a fall of approximately 109.62/74.81 cm^{-1} in carbonyl frequency for acetyl group.

As for the $\nu(C=N)$ stretching modes of thiazole ring of the title molecule observed at 1510.28 cm^{-1} was calculated as 1498.29/1528.25 cm^{-1} at the B3LYP and HSEH1PBE /LanL2DZ levels respectively, which are coupled by $\nu(C-C)$ stretching vibration. Furthermore, the $\nu(C-N)$ stretching modes observed at 1446.61 and 1269.52 cm^{-1} and calculated at the mentioned levels as 1444.87/1448.45 and 1223.73/1252.40 cm^{-1}, respectively. On the other hand, the $\nu(S-C)$ stretching mode is observed at 667.37 cm^{-1} as a strong band in Fig. 2 and calculated as 667.11/678.55 cm^{-1} at the mentioned levels, respectively.

3.3. NMR analysis

The nuclear magnetic resonance (NMR) spectroscopy is a powerful tool for determining the composition, structure and

TABLE III. The calculated 1H and 13C NMR chemical shifts (ppm) at the B3LYP and HSEH1PBE/LanL2DZ levels for 5-acetyl-2,4-dimethylthiazole.

| Atom	B3LYP		HSEH1PBE	
	Gas	Chloroform	Gas	Chloroform
1H				
H7	1.3815	1.5944	1.4394	1.6537
H8	1.3814	1.5947	1.4394	1.6539
H9	2.2407	2.1332	2.3638	2.2579
H12	1.5738	1.7628	1.6497	1.8438
H13	1.5737	1.7628	1.6496	1.8438
H14	1.6947	1.6557	1.8062	1.7659
H16	1.5028	1.7462	1.5678	1.8121
H17	1.5029	1.7464	1.5678	1.8122
H18	1.6591	1.612	1.7869	1.7451
^{13}C				
C1	200.949	187.451	177.924	181.027
C2	163.942	150.971	142.059	145.673
C3	170.241	152.296	146.952	145.706
C6	31.2081	14.7945	10.3229	10.490
C10	206.325	194.838	185.19	190.306
C11	31.9947	15.5823	11.0375	11.2336
C15	42.5408	26.3812	21.5967	22.0522

function of complex molecules and to compute the reliable magnetic properties which provide the accurate predictions of molecular geometries and the isotropic chemical shift analysis [37,38]. In this framework, the ^{1}H and ^{13}C NMR chemical shift values were calculated at the mentioned levels by using GIAO model. The calculated ^{1}H and ^{13}C NMR chemical shift values of the title molecule in gas phase and in the chloroform solvent at the B3LYP and HSEH1PBE /LanL2DZ levels are presented in Table III.

By considering Table III, the outstanding point for the calculated ^{1}H NMR chemical shift values in CHCl$_3$ solvent is that the all computed values vary at the interval 1.5944/1.6537-2.1332/2.2579 ppm at the B3LYP and HSEH1PBE /LanL2DZ levels since all protons of the 5-acetyl-2,4-dimethylthiazole compound (C$_7$H$_9$NOS) which has no aromatic ring proton belongs to the methyl groups.

On the other hand, as seen in Table III, the highest calculated carbon-13 NMR chemical shift value in CHCl$_3$ solvent of the title molecule at the B3LYP and HSEH1PBE /LanL2DZ levels was found as 194.838/190.306 ppm for the C10 atom which is connected to the O19 atom with high electronegativity while the lowest two calculated values in the chloroform solvent were found as 14.7945/10.49 ppm and 15.5823/11.2336 ppm for the C6 and C11 atoms, respectively.

TABLE IV. The experimental (in chloroform solvent) and calculated electronic transitions and oscillator strengths of 5-acetyl-2,4-dimethylthiazole at the B3LYP and HSEH1PBE/LanL2DZ levels.

Transition	Experimental	B3LYP						HSEH1PBE					
	Chloroform	Gas			Chloroform			Gas			Chloroform		
	λ (cm)	λ (cm)	E (eV)	Osc.	λ (cm)	E (eV)	Osc.	λ (cm)	E (eV)	Osc.	λ (cm)	E (eV)	Osc.
		370.15	3.3495	0.0000	360.07	3.4434	0.0001	361.36	3.4310	0.0001	352.88	3.5288	0.0001
$n \rightarrow \pi*$	278	268.95	4.6099	0.1865	277.46	4.4685	0.2667	261.20	4.7468	0.2107	269.74	4.5964	0.2929
$\pi \rightarrow \pi*$	265	247.46	5.0103	0.1183	251.02	4.9391	0.1360	239.41	5.1788	0.1117	242.69	5.1087	0.1312
$\pi \rightarrow \pi*$	243	217.83	5.6918	0.0014	214.33	5.7849	0.0020	210.96	5.8771	0.0016	207.75	5.9678	0.0022
		205.32	6.0386	0.0003	205.91	6.0212	0.0004	198.89	6.2337	0.0002	199.47	6.2157	0.0003
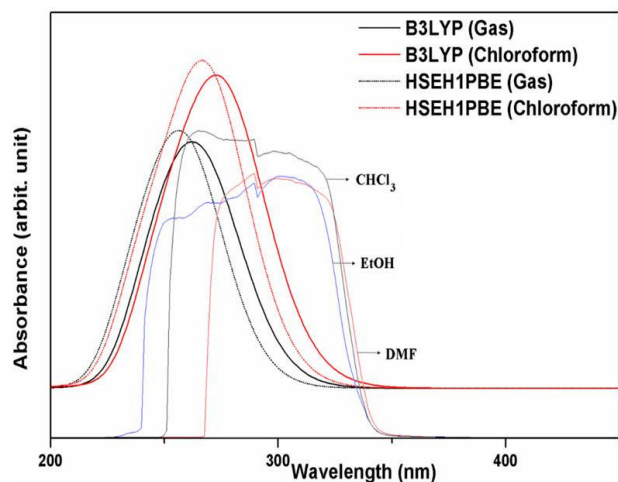
FIGURE 3. The experimental (in CHCl$_3$, EtOH and DMF) solvents and simulated UV-vis spectra at the B3LYP and HSEH1PBE/LanL2DZ levels.

3.4. UV-vis absorption and FMOs analysis

The experimental UV-vis in ethanol (EtOH), chloroform (CHCl$_3$) and N, N-dimethylformamide (DMF) solvents and the simulated at the B3LYP and HSEH1PBE/LanL2DZ levels in gas phase and chloroform solvent spectra of the 5-acetyl-2,4-dimethylthiazole molecule are presented in Fig. 3. Furthermore, the maximum absorption wavelengths (λ_{max}), excitation energies and oscillator strengths calculated by using TD-DFT/ B3LYP and HSEH1PBE/LanL2DZ levels of the title molecule in both gas and chloroform solvent are presented in Table IV.

The experimental maximum absorption wavelengths (λ_{max}) are observed at 243 nm, 265 nm, 278 nm, 295 nm and 315 nm in ethanol solvent, 259 nm, 295 nm, 309 nm, 318 nm and 337 nm in chloroform solvent and 295 nm and 316 nm in N, N-dimetylformamide solvent. By considering Table IV, the calculated maximum absorption wavelengths (λmax) in chloroform solvent which correspond to the experimental 278, 265 and 243 nm λ_{max} values in chloroform solvent were found as 277.46/269.74 nm, 251.02/242.69 nm and 214.33/207.75 nm at the B3LYP and HSEH1PBE/LanL2DZ

levels, respectively. Therefore, the observed and calculated absorption bands can be attributed to the $\pi \rightarrow \pi*$, $\pi \rightarrow \pi*$ and $n \rightarrow \pi*$ transitions for the title molecule [39].

On the other hand, the highest occupied molecular orbital (HOMO) and the lowest unoccupied molecular orbital (LUMO) called the frontier molecule orbitals (FMOs) mean the outermost orbital filled by electrons and the first empty innermost orbital unfilled by electron, respectively. The HOMO is directly related to the ionization potential and behaves as an electron donor and the LUMO is directly related to the electron affinity and behaves as an electron acceptor. Therefore, the energy gap formed between HOMO and LUMO can be considered as a critical parameter and is an indicator in terms of the molecular chemical stability, and to identify the molecular electrical transport properties of any molecule. By using this energy gap, the molecular properties such as the chemical reactivity, polarizability, chemical hardness and softness, and electronegativity can be determined [40,41].
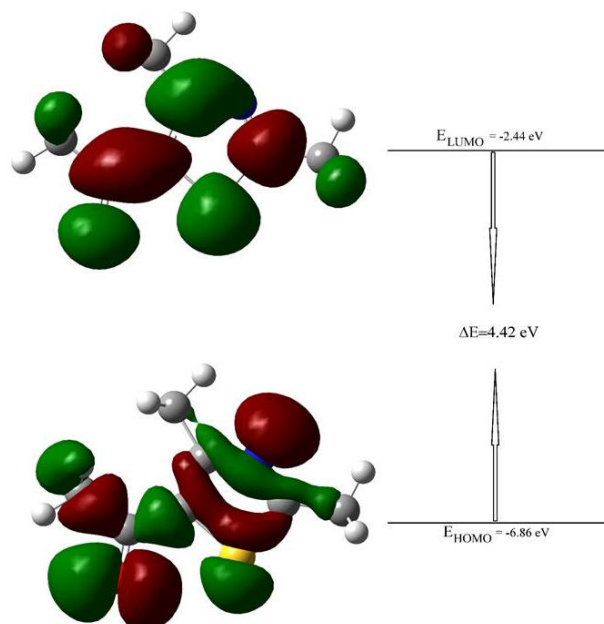

FIGURE 4. 3D plots of HOMO-LUMO of 5-acetyl-2,4-dimethyl thiazole at the HSEH1PBE/LanL2DZ level.

TABLE V. Second-order perturbation theory analysis of Fock matrix in NBO basic corresponding to the intramolecular bonds of 5-acetyl-2,4-dimethylthiazole calculated at the B3LYPand HSEH1PBE/LanL2DZ levels.

Donor (i)	ED(i) (e)		Acceptor (j)	ED(j) (e)		E(2)^a (kcal/mol)		E(j)-E(i)^b (a.u.)		F(i,j)^c (a.u.)	
	B3LYP	HSEH1PBE		B3LYP	HSEH1PBE	B3LYP	HSEH1PBE	B3LYP	HSEH1PBE	B3LYP	HSEH1PBE
$\sigma(C_3$-$S_4)$	1.96	1.96	$\sigma*$ $(C_2$-$C_6)$	0.02	0.02	7.01	7.17	0.94	0.96	0.074	0.073
$\sigma(C_{11}$-$N_6)$	1.98	1.98	$\sigma*$ $(C_2$-$S_4)$	0.96	0.94	7.19	7.41	0.70	0.71	0.064	0.066
LP1 (N_5)	1.89	1.89	$\sigma*(C_2$-$C_3)$	0.04	0.04	8.46	8.63	0.89	0.90	0.079	0.080
$\pi(C_2$-$C_3)$	1.79	1.79	$\pi*$ $(C_1$-$N_5)$	0.32	0.33 1	0.20	9.73	0.27	0.27	0.049	0.047
LP2 (O_{19})	1.90	1.91	$\sigma*$ (C3-C10)	0.06	0.06	15.61	15.79	0.69	0.70	0.094	0.095
LP2 (S_4)	1.64	1.63	$\pi*$ (C2-C3)	0.30	0.31	15.69	15.12	0.26	0.26	0.058	0.057
LP2 (O_{19})	1.90	1.91	$\sigma*(C_{10}$-$C_{15})$	0.05	0.05	17.26	17.42	0.61	0.62	0.093	0.094
LP1(N_5)	1.89	1.89	$\sigma*(C_1$- $S_4)$	0.09	0.09	17.43	17.15	0.54	0.55	0.087	0087
π (C_1-N_5)	1.85	1.85	$\pi*(C_2$ - $C_3)$	0.30	0.31	19.59	19.38	0.34	0.34	0.076	0.076
$\pi(C_2$-$C_3)$	1.79	1.79	$\pi*(C_{10}$-$O_{19})$	0.18	0.18	24.10	23.62	0.28	0.28	0.074	0.073
LP2 (S_4)	1.64	1.63	$\pi*$ $(C_1$-$N_5)$	0.32	0.33	27.47	26.74	0.23	0.23	0.072	0.070

ED = electron density; ^{a}E(2) means energy of hyperconjugative interaction (stabilization energy); ^{b}Energy difference between donor and acceptor i and j NBO orbitals; ^{c}F(i, j) is the Fock matrix element between i and j NBO orbitals.

In this study, the 3-dimensional (3D) plots of the title molecule at the HSEH1PBE /LanL2DZ level are given in Fig. 4. The calculated energy gap value between the HOMO-LUMO for the title molecule is 4.42 eV at the mentioned level, as seen in Fig. 4. The large energy gap demonstrates the charge transfer occurs within of the title compound, and complex cannot be easily polarized. Besides, this value showing HOMO $\rightarrow$ LUMO contribution is originated from $\pi \rightarrow \pi*$ transition, as seen in Table IV and Fig. 4.

3.5. NBO analysis

The NBO analysis provides an explanation of the intramolecular and intermolecular bondings and interactions among bonds in molecular system. Furthermore, it allows to study on the hyperconjugation interactions or charge transfers (ICT) in the molecules.

In this framework, a stabilizing donor-acceptor interaction is corresponded to the delocalization of electron density between occupied Lewis type orbitals and formally unoccupied non-Lewis orbitals. Therefore, in order to make clear the intra- and inter-molecular interactions in the molecular systems, the stabilization energies of the molecules have been studied by using second-order perturbation theory. For each donor NBO (i) and acceptor NBO (j), the stabilization energy $E^{(2)}$ associated with electron delocalization between donor and acceptor is estimated as [42,43]

$$E^{(2)} = -q_i \frac{F_{ij}^2}{\Delta E} = -q_i \frac{\langle i|F|j\rangle^2}{\varepsilon_j - \varepsilon_i} \qquad (1)$$

where q_i is the donor orbital occupancy, ε_i and ε_j are diagonal elements (orbital energies), and F_{ij} is the off-diagonal NBO Fock matrix element (1). In this work, the results of second-order perturbation theory analysis of the Fock Matrix

at the B3LYP and HSEH1PBE /LanL2DZ levels of theory for the 5-acetyl-2,4-dimethylthiazole molecule is presented in Table V.

By considering Table V, the stabilization energy values greater than 7.00 kcal mol^{-1} are listed. Therefore, the strongest stabilization energy values calculated at the B3LYP and HSEH1PBE/LanL2DZ levels were found as 27.47/26.74 kcal/mol, respectively and corresponds to the transition between the lone pair n electrons of S4 electrons and $\pi*$ antibonding electrons of the C1-N5 in thiazole ring. Furthermore, the transitions between n(N5)$\rightarrow$ $\sigma*$(C1-S4), n(O19)$\rightarrow$ $\sigma*$ (C10-C15) and n(O19)$\rightarrow$ $\sigma*$(C3-C10) occurred in the title molecule. Likewise, the $\pi \rightarrow \pi*$ transition occurred between (C2-C3) and (C10-O19) bonds for the title molecule, as seen in Table V.

3.6. NLO parameters

The calculated results of the molecular polarizabilities at the B3LYP and HSEH1PBE /LanL2DZ levels of the finite-field approach for the 5-acetyl-2,4-dimethylthiazole molecule are given in Table VI. Therefore, total static dipole moment μ, the mean polarizability $<\alpha>$, the anisotropy of the polarizability $\Delta\alpha$ and the mean first hyperpolarizability $<\beta>$ which form the molecular polarizabilities of the title compound are shown in Table VI. As seen in Table VI, the μ in Debye, $<\alpha>$ and $\Delta\alpha$ in 10^{-24} esu, and $<\beta>$ in 10^{-30} esu are presented as defined in cited [44].

Therefore, the calculated values at the B3LYP and HSEH1PBE /LanL2DZ levels converted by using $1 a.u = 0.1482 \times 10^{-24}$ electrostatic unit (esu) for α and $1 a.u = 8.6393 \times 10^{-33}$ esu for β are reported as the polarizabilities and hyperpolarizability, respectively. On the other hand, it is well-known that the $<\beta>$ value is a crucial factor for the

TABLA VI. Total dipole moment (μ, in Debye), the mean polarizability ($< \alpha >$, in 10^{-24} esu), the anisotropy of the polarizability ($\Delta\alpha$, in 10^{-24} esu), the mean first-order hyperpolarizability ($< \beta >$, in 10^{-30} esu) for 5-Acetyl-2,4-dimethylthiazole calculated at the B3LYPand HSEH1PBE/LanL2DZ levels.

Property	B3LYP	HSEH1PBE
μ	3.10	3.09
$< \alpha >$	14.46	14.31
$\Delta\alpha$	10.45	10.13
$< \beta >$	3.38	3.32
$< \beta > *$	0.37289	

* Taken from Ref. [44].
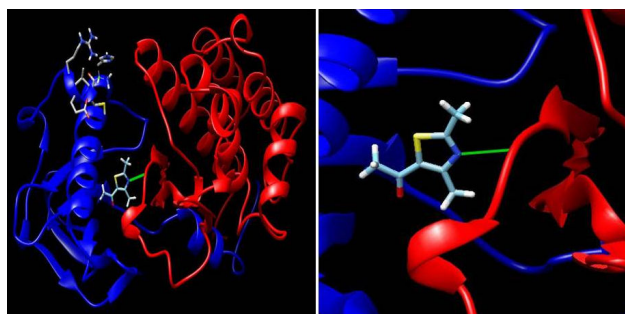
FIGURE 5. Binding model of 5-acetyl-2,4-dimethylthiazole with VEFGR-2 (PDB ID: 2XIR)

NLO parameters of the molecular systems and in this work, the calculated $< \beta >$ values for the title molecule were found as $3.38/3.32 \times 10^{-30}$ esu at the mentioned levels, as seen in Table VI.

3.7. Molecular Docking

The binding properties of 5-acetyl-2,4-dimethylthiazole to the VEGFR-2 kinase (PDB ID: 2XIR) and acetoacetyl-ACP synthase (PDB ID: 1HNJ) proteins were investigated, and molecular modelling studies were performed for ligand-protein interactions. Molecular docking studies provide the best representation of the association of the studied compound with the receptor, as well as hydrogen bonds that play an important role in ligand-protein interaction which is required for inhibition activity. As a result of the molecular docking studies, it was found that the optimized structure of the 5-acetyl-2,4-dimethylthiazole binds to the protein by hydrogen bonding with certain amino acids in the binding region of both proteins. The obtained energy and hydrogen bond location informations are given in Table VII.

According to the results, in the most stable docked pose between ligand-2XIR showed lowest interaction energy of -6.02 kcal/mol and was involved a hydrogen bonding interaction with Asp 1046 in the active site of 2XIR (Fig. 5). The amino acid Asp1046 had formed hydrogen bonding with nitrogen atom of 5-acetyl-2,4-dimethylthiazole (2.038 Å).

TABLE VII. Full fitness score, binding energy and hydrogen bond information between the ligand-target molecule couples.

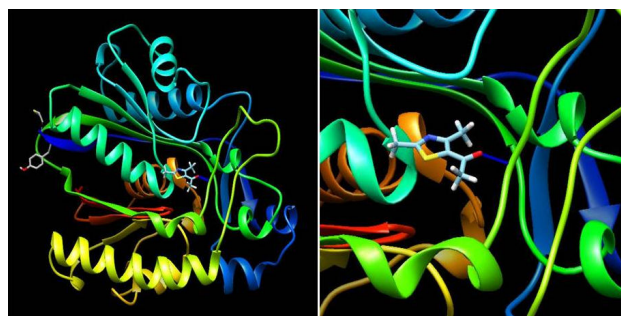| Ligand-Target	Full fitness score (kcal/mol)	ΔG (kcal/mol)	H Bond Location (Length)
Ligand-2XIR	-1631.80	-6.02	N of ligand & NH of Asp 1046 (2.038 Å)
Ligand-1HNJ	-1435.90	-5.96	O of ligand & NH of Leu 191 (2.165 Å)

FIGURE 6. Binding model of 5-acetyl-2,4-dimethylthiazole with KAS III (PDB ID: 1HNJ).
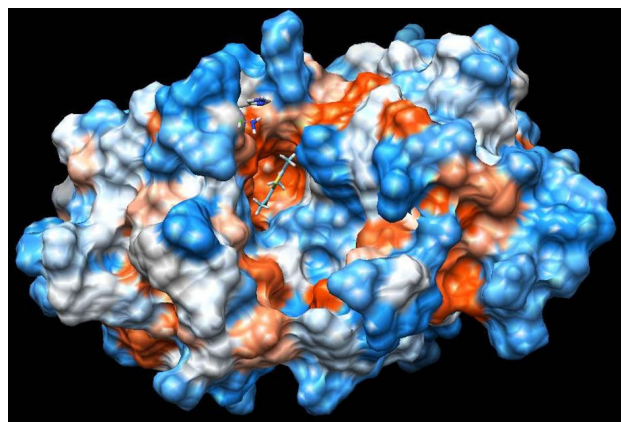

FIGURE 7. The binding of 5-acetyl-2,4-dimethylthiazole in the active site of VEFGR-2 (PDB ID: 2XIR).

On the other hand, ligand-1HNJ interaction exhibited the higher free energy at -5.96 kcal/mol than the ligand-2XIR couple. 5-Acetyl-2,4-dimethylthiazole and 1HNJ interaction also exhibited a hydrogen bonding between O atom of ligand and NH of Leu 191 with a 2.165 Å bond length (Fig. 6). Since the ligand forms a shorter hydrogen bonding with the 2XIR, the bond between the two is much stronger than ligand-1HNJ couple. Full fitness score value of ligand-2XIR (Fig. 7) and ligand-1HNJ (Fig. 8) interactions were found to be as -1631.80 and -1435.90 kcal/mol, respectively. These scores were in accordance with the order of the binding energy values. Docking assay of 5-acetyl-2, 4-dimethylthiazole with
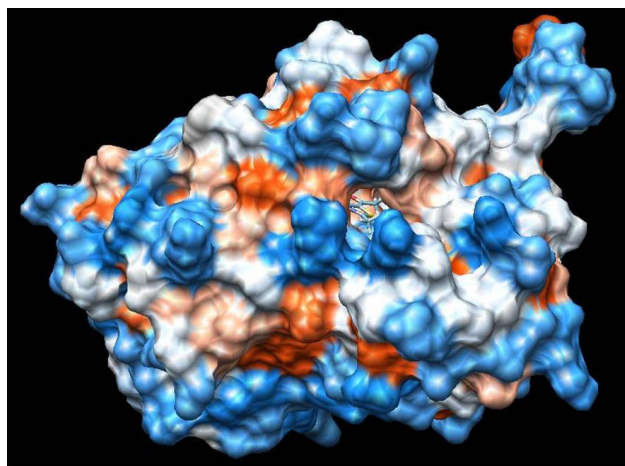
FIGURE 8. The binding of 5-acetyl-2,4-dimethylthiazole in the active site of KAS III (PDB ID: 1HNJ).

2XIR showed a better full fitness score value and more preferred interaction.

The docking study results clearly reveal that 5-acetyl-2,4-dimethylthiazole showed strong binding affinity towards the target proteins, achieving the best full fitness score and binding energy against 2XIR. However, full fitness score and binding energy for 1HNJ also appeared significant. On the basis of docking results, it was found that 5-acetyl-2,4-dimethylthiazole had potential to inhibit vascular endothelial growth factor receptor-2 kinase and β-Ketoacyl-acyl carrier protein synthase III.

4. Conclusion

The present work indicates that the calculations on the 5-acetyl-2,4-dimethylthiazole molecule give us a reliable assignment for the NMR, IR and UV-vis spectra of the molecule. Meanwhile, the results of NBO analysis for title molecule exhibit that the calculated strongest stabilization energy values in $n \rightarrow \pi*$ and $\pi \rightarrow \pi*$ transitions were confirmed by the observed data obtained from the experimental UV-vis. spectrum in the chloroform solvent. The study of the HOMO-LUMO analysis at the HSEH1PBE /LanL2DZ level in this work confirms the $\pi \rightarrow \pi*$ transition for the 5-acetyl-2,4-dimethylthiazole molecule. Furthermore, computer aided ligand binding studies identified possible interactions and binding poses of 5-acetyl-2,4-dimethylthiazole with the VEGFR-2 and KAS III. The docking result revealed that ligand formed more strongly hydrogen bond interaction with active residues of VEGFR-2. The structure of proteins is important for their functions in the biological environment. The conformations of proteins are effective in determining binding molecules and binding force. The region where the ligand will be bound to the protein is closely related to the shape, size, charge, hydrophilic and hydrophobic properties of the ligand. In molecular doking studies, the most stable geometric structure of the 5-acetyl-2,4-dimethylthiazole ligand obtained by DFT calculations was used and low full fitness scores were obtained. This result showed that the active site of the proteins and the ligand were quite compatible. Furthermore, the small HOMO-LUMO gap of the ligand means that this molecule was soft and reactive in chemical reactions. The reason why the title molecule interacts highly with both proteins used in the molecular docking study may be the high reactivity of the molecule due to its softness. As a result, we can say that 5-acetyl-2,4-dimethylthiazole could be used as potential compound for developing antitumor agents. However, biological tests need to be performed to confirm the molecular docking predictions.

1. W. Risau, *Nature* **386** (1997) 671.

2. F. Shalaby, J. Rossant, T. P. Yamaguchi, M. Gertsenstein, X.F. Wu, M.L. Breitman, A.C. Schuh, *Nature* **376** (1995) 62.

3. N. Ferrara, H. P. Gerber, J. LeCouter, *Nat. Med.* **9** (2003) 669.

4. M. Shibuya, L. Claesson-Welsh, *Exp. Cell Res.* **312** (2006) 549.

5. J. C. Harmange, *et al*. *Med. Chem.* **51** (2008) 1649.

6. K. J. Kim, B. Li, J. Winer, M. Armanini, N. Gillett, H. S. Phillips, N. Ferrara, *Nature* **362** (1993) 841.

7. B. Karaman, N. Ulusoy Güzeldemirci, *Med. Chem. Res.* **25** (2016) 2471.

8. M. H. Sherif, I. M. Eldeen, E. O. Helal, *Res. Chem. Intermed.* **39** (2013) 3949.

9. C. Y. Lai, J. E. Cronan, *J. Biol. Chem.* **278** (2003) 51494.

10. F. Jensen, *Introduction to Computational Chemistry* (John Wiley & Sons Inc.:New York, 1974).

11. P. Pulay, *Mol. Phys.* **17** (1969) 197.

12. J. P. Perdew, In *Proceedings of the 21st Annual Symposium on the Electronic Structure of Solids*, 91; P. Ziesche, H. Eschig, (Eds.; Akademie Verlag: Berlin, 1991).

13. J. P Perdew, Y. Wang, *Phys. Rev. B*. **45** (1992) 13244.

14. A. D. Becke, *J. Chem. Phys.* **98** (1993) 5648.

15. C. Lee, W. Yang, R. G. Parr, *Phys. Rev. B* **37** (1988) 785.

16. K. Burke, J. P. Perdew, Y. Wang, *In Electronic Density Functional Theory: Recent Progress and New Directions*; J.F. Dobson, G. Vignale, M.P. Das, Eds.; Plenum:New York, 1998.

17. Y. Zhao, J. Pu, B. J. Lynch, D. G Truhlar, *Phys. Chem. Chem. Phys.* **6** (2004) 673.

18. J. Heyd, G. E. Scuseria, M. J. Ernzerhof, *J. Chem. Phys.* **124** (2006) 219906.

19. D. Avcı, B. Dede, S. Bahçeli, D. Varkal, *J. Mol. Struct.* **1138** (2017) 110.

20. Gaussian 09, Revision C.01, M. J. Frisch, *et al.*, Inc., Wallingford CT, (2009).

21. GaussView, Version 5, Roy Dennington, Todd Keith and John Millam, Semichem Inc., Shawnee Mission KS, 2009.

22. J. B. Foresman, E. Frisch, *Exploring Chemistry with Electronic Structure Methods*, Gaussian, Inc., Pittsburgh, PA, USA, 1993.

23. M. L. Laury, M .J. Carlson, A. K. Wilson, *J. Comput. Chem.* **33** (2012) 2830.

24. D. Avc, S. Bahçeli, Ö. Tamer, Y. Atalay, *Can. J. Chem.* **93** (2015) 1.

25. M. H. Jamr'oz, *Vibrational Energy Distribition Analysis VEDA4*, Warsaw, 2004.

26. F. London, *J. Phys. Radium* **8** (1937) 397.

27. K. Wolinski, J. F. Himton, P. Pulay, *J. Am. Chem. Soc.* **112** (1990) 8251.

28. R. Bauernschmitt, R. Ahirichs, *Chem. Phys. Lett.* **256** (1996) 454.

29. C. Jamorski, M. E Casida, D. R. Salahub, *J. Chem. Phys.* **104** (1996) 5134.

30. A. Grosdidier, V. Zoete, O. Michielin, *Nucleic Acids Res.* **39** (2011) W270.

31. E. F. Pettersen *et al.*, *J. Comput. Chem.* **13** (2004) 1605.

32. N. B. Colthup, L. H. Daly, E. Wiberley, *Introduction to Infrared and Raman Spectroscopy*, (Academic Press, New York, 1964).

33. L. J. Bellamy, *The Infrared Spectra of Complex Molecules*, 3rd edition, Wiley, (New York, 1975).

34. J. B. Lambert, H. F. Shurvell, R .G. Cooks, *Introduction to Organic Spectroscopy*, Macmillan Publishing, New York, Chapter 7, p174, (1987).

35. B. H. Stuart, *Infrared Spectroscopy: Fundamentals and Applications*, JohnWilley & Sons, England, 2004.

36. R. M. Silverstein, F. X. Webster, *Spectroscopic Identification of Organic Compound*, (6nd edn), (John Willey & Sons, New York, 1998).

37. L. G. Wade, *Organic Chemistry*, Pearson Prentice Hall, (New Jersey, 2006).

38. H. O. Kalinowski, S. Berger, S. Braun, *Carbon-13 NMR Spectroscopy*, (John Wiley & Sons Ltd., Chichester, UK, 1988).

39. N. Süleymano?lu, R. Ustabas¸ Y. B. Alpaslan, F. Eyduran, N. O. Iskeleli, *Spectrochim. Acta Part A* **96** (2012) 35.

40. K. Fukui, *Science* **218** (1982) 747.

41. H. Gökce, S. Bahçeli, *Spectrochim. Acta Part A* **79** (2011) 1783.

42. A. Pirnau, V. Chi?, O. Oniga, N. Leopold, L. Szabo, M. Baias, O. Cozar, *Vib. Spectrosc.* **48** (2008) 289.

43. C. James, A. A. Raj, R. Reghunatan, V. S. Jayakumar, I. H. Joe, *J. Raman Spectrosc.* **37** (2006) 1381.

44. Y.-X. Sun, Q.-L. Hao, W.-X. Wei, Z.-X. Yu, L.-D. Lu, X. Wang, Y.-S. Wang, *J. Mol. Struct. (THEOCHEM)* **904** (2009) 74.